

Evolution of phase separation in In-rich InGaN alloys

B. N. Pantha, J. Li, J. Y. Lin, and H. X. Jiang^{a)}

Department of Electrical and Computer Engineering, Texas Tech University, Lubbock, Texas 79409, USA

(Received 20 March 2010; accepted 16 May 2010; published online 11 June 2010)

Evolution of phase separation in $\text{In}_x\text{Ga}_{1-x}\text{N}$ alloys ($x \sim 0.65$) grown on AlN/sapphire templates by metal organic chemical vapor deposition has been probed. It was found that growth rate, G_R , is a key parameter and must be high enough ($>0.5 \mu\text{m/h}$) in order to grow homogeneous and single phase InGaN alloys. Our results implied that conditions far from thermodynamic equilibrium are needed to suppress phase separation. Both structural and electrical properties were found to improve significantly with increasing G_R . The improvement in material quality is attributed to the suppression of phase separation with higher G_R . The maximum thickness of the single phase epilayer t_{max} (i.e., maximum thickness that can be grown without phase separation) was determined via *in situ* interference pattern monitoring and found to be a function of G_R . As G_R increases, t_{max} also increases. The maximum value of t_{max} for $\text{In}_{0.65}\text{Ga}_{0.35}\text{N}$ alloy was found to be $\sim 1.1 \mu\text{m}$ at $G_R > 1.8 \mu\text{m/h}$. © 2010 American Institute of Physics. [doi:10.1063/1.3453563]

The determination of true band gap of InN around 0.7 eV (Refs. 1–3) has extended the energy gap range of group III-nitrides from deep ultraviolet to the near infrared spectral region. In particular, the band gap energy of $\text{In}_x\text{Ga}_{1-x}\text{N}$ alloys can be continuously varied from 0.7 to 3.4 eV, covering the entire solar spectrum. This opens up the possibility for realizing a full spectrum solar cell. Many groups are exploring the potential of InGaN as solar cell materials.^{4–8} Besides being the ideal photovoltaic materials, In-rich InGaN alloys have also attracted considerable attention for their potential applications in long wavelength emitters, photoelectrochemical cells, and thermoelectric devices.^{9–12} In an effort to synthesize high quality In-rich InGaN alloys, many growth techniques have been tried.^{12–17} Nonetheless, there remains considerable difficulty in making high-quality In-rich InGaN alloys, mainly due to phase separation.

Very thin InGaN layers (on the order of few nanometers) in the form of single or multiple quantum wells are used as active layers in InGaN based blue green light emitting diodes (LEDs) and laser diodes (LDs). The realization of high brightness LEDs and LDs is predominately attributed to the incorporation of high quality thin layers of InGaN with relatively low In-contents.¹⁸ The material quality of InGaN with high In-contents severely degrades due to phase separation, inhomogeneity of solid solution, and In metal droplets (due to decomposition of InN) as layer thickness increases. Phase separation in In-rich InGaN has been theoretically predicted and experimentally observed in thick layers.^{19,20} Most of the aforementioned applications need high In-content InGaN layers that are much thicker than those employed in quantum wells in order to realize practical devices. Growth of such high In-content and thick InGaN alloy layers inside the theoretically predicted miscibility gap region has proven to be very challenging. However, some progresses have been made recently in the growth of single phase InGaN alloys in the entire compositional range.^{13,14} Nakamura *et al.*¹⁸ has experimentally shown that the quality of InGaN films can be improved by reducing the growth rate in low In-content regime. However, we found that such a low growth rate inside the

theoretically predicted miscibility gap region (middle range of the alloy composition) has resulted in phase separation and poor electrical and structural properties. Here, we report on an effective method to suppress phase separation and improve the crystalline quality of In-rich InGaN alloys. In particular, the evolution of the miscibility gap with the layer thickness and growth rate (G_R) has been investigated in $\text{In}_{0.65}\text{Ga}_{0.35}\text{N}$ alloy.

$\text{In}_x\text{Ga}_{1-x}\text{N}$ alloys ($x \sim 0.65$) were grown on AlN/sapphire templates by metal organic chemical vapor deposition. A thin $\text{In}_{0.2}\text{Ga}_{0.8}\text{N}$ buffer layer ($\sim 20 \text{ nm}$) was grown prior to the growth of the epilayers. Trimethylgallium (TMGa), trimethylindium (TMIn), and ammonia (NH_3) were used for Ga, In, and N sources, respectively. Growth temperature and pressure were fixed at $610 \text{ }^\circ\text{C}$ and 500 Torr, respectively. Growth rate was increased by increasing flow rate of group III sources with a constant TMIn/TMGa ratio. Electrical and structural properties were measured by Hall-effect and x-ray diffraction (XRD), respectively. In-fractions in InGaN epilayers were also checked by secondary ion mass spectrometry (by Evans Analytical Group) for selective samples, which revealed that In-contents determined by XRD are in very good agreement with secondary ion mass spectrometry results.

Figure 1(a) shows the XRD spectra for (002) plane in θ - 2θ scan mode. In-contents were determined from the peak angles using the Vegard law with the assumption that layers are fully relaxed as they are thick enough ($\sim 300 \text{ nm}$). In this figure, right peaks correspond to the InGaN buffer layer while left peaks are from the top InGaN layer. Indium contents in buffer and top layers were found to be $\sim 20\%$ and 65% , respectively. At $R_G \sim 0.2 \mu\text{m/h}$, a very broad peak was observed which corresponds to In content between $\sim 35\%$ and 65% . This is due to the inhomogeneity and phase separation. As G_R increases, phase separation and inhomogeneity are gradually suppressed, as evidenced by the emergence of a single peak from the top $\text{In}_x\text{Ga}_{1-x}\text{N}$ ($x \sim 0.65$) layer. Slight shift in the main peak toward a smaller angle is due to a higher In incorporation with an increase in G_R . Effect of G_R on In incorporation is more prominent for the growth of lower In-content InGaN alloys, as shown in Fig.

^{a)}Electronic mail: hx.jiang@ttu.edu.

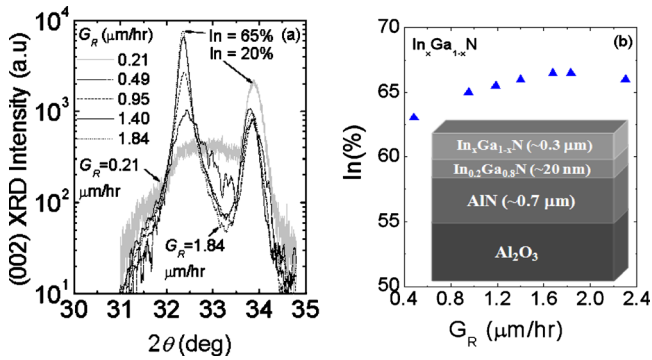


FIG. 1. (Color online) (a) XRD spectra of (002) θ -2 θ scan of $\text{In}_x\text{Ga}_{1-x}\text{N}$ ($x \sim 0.65$) alloys grown at different growth rate G_R . (b) In content as a function of growth rate G_R with fixed growth temperature $T_G = 610^\circ\text{C}$ and pressure $P = 500$ Torr. Layer structure is shown in the inset.

1(b). Figure 1(b) shows that In content is nominally increased with an increase in G_R . The inset of Fig. 1(b) shows the layer structure. Since epilayers are thick, effect of strain in suppressing phase separation is expected to be negligible.

Structural property dependence on G_R is plotted in Figs. 2(a) and 2(b). It is found that as G_R increases, full-width at half maxima (FWHM) of XRD spectra decrease and XRD intensity increase for both (002) θ -2 θ scans and rocking curves (ω -2 θ scans). FWHM of θ -2 θ scans (rocking curves) decreased from $\sim 0.64^\circ$ (3.06) to $\sim 0.19^\circ$ (1.02) when G_R increased from ~ 0.5 to 1.4 $\mu\text{m}/\text{h}$. FWHM of θ -2 θ scans indicate degree of homogeneity of alloys, while FWHM of rocking curves (or ω -2 θ scans) reveal the crystalline quality. Further increases in G_R only moderately improve the film's structural properties. This infers that once single phase and homogeneous alloy are attained, structural properties remain almost independent of G_R . The narrowest FWHM for (002) θ -2 θ and rocking curve were measured to be 648 arc sec and 3240 arc sec, respectively when $G_R = 1.8$ $\mu\text{m}/\text{h}$. FWHM of (002) θ -2 θ curves are much narrower than those we reported previously in InGaN with similar In-contents.¹³ Our results suggest that G_R needs to be greater than 1.0 $\mu\text{m}/\text{h}$ to obtain single phase $\text{In}_{0.65}\text{Ga}_{0.35}\text{N}$ with reasonable homogeneity and crystalline quality.

Electrical properties, electron mobility (μ_e) and background concentration (n), of $\text{In}_{0.65}\text{Ga}_{0.35}\text{N}$ alloys as a function of G_R are plotted in Fig. 3. It was found that μ_e increases with G_R . Electron mobility increases from 44 to 90 cm^2/Vs , almost linearly, when G_R is increased from ~ 0.5 to 1.4 $\mu\text{m}/\text{h}$ and then remains almost the same with

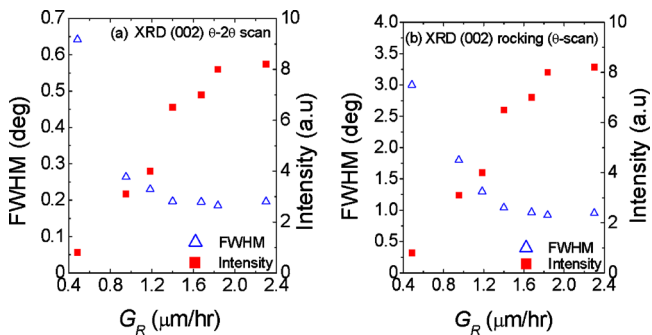


FIG. 2. (Color online) FWHM and intensity of XRD curves of (002) plane in (a) θ -2 θ (b) rocking curves of $\text{In}_{0.65}\text{Ga}_{0.35}\text{N}$ alloy as functions of growth rate, G_R .

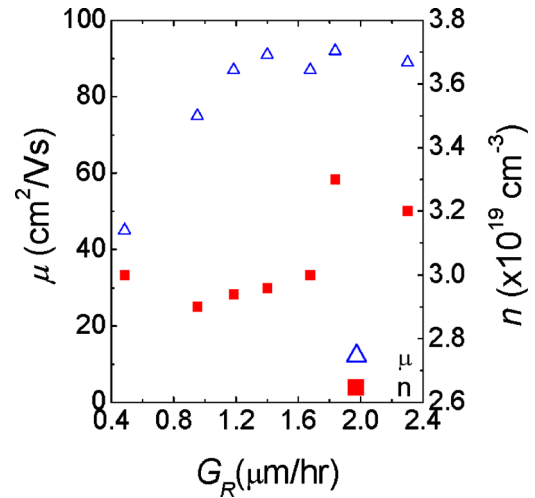


FIG. 3. (Color online) Electron mobility μ_e and concentration n of $\text{In}_{0.65}\text{Ga}_{0.35}\text{N}$ alloy as functions of growth rate G_R .

further increase in G_R . We have observed that both XRD and Hall results are improved with increasing G_R . Electron mobility has increased by more than a factor of 2 when G_R was increased from 0.5 to 1.4 $\mu\text{m}/\text{h}$ while n remained the same, although very high. The physical origin of such a high n ($\sim 3 \times 10^{19} \text{cm}^{-3}$) is currently under intensive investigation and impurities such as hydrogen or nitrogen vacancies could be responsible for such high n .^{21,22} Detailed dependence of other growth parameters such as V/III ratio, pressure, temperature, etc., and strain management would eventually provide us with understanding as well as mechanisms to control n .

Figure 4(a) shows the evolution of *in situ* interference patterns with varying G_R during growth of $\text{In}_{0.65}\text{Ga}_{0.35}\text{N}$ alloy. It was found that reflected laser intensity decreased abruptly as layer thickness exceeded a certain value. The surface of the epilayer started getting rough at this point. XRD results indicate that the InGaN samples with such an interference pattern were phase separated with pure InN phase having In droplets on the surface. At $G_R = 1.8$ $\mu\text{m}/\text{h}$, we did not see such an abrupt drop in laser intensity until the layer exceeds 1.1 μm thick before phase separation occurred, as shown at the bottom most spectrum of Fig. 4(a). Thus, the reason for the abrupt decrease in laser beam intensity is most likely due to the bad surface caused by In drop-

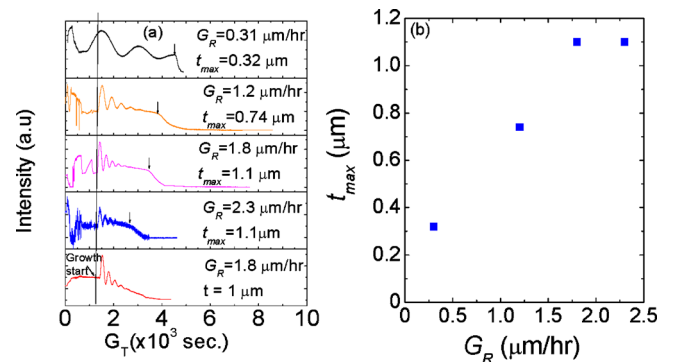


FIG. 4. (Color online) (a) *In situ* interference spectra of $\text{In}_{0.65}\text{Ga}_{0.35}\text{N}$ alloys during growth and (b) maximum thickness t_{max} of $\text{In}_{0.65}\text{Ga}_{0.35}\text{N}$ that can be grown without phase separation, as a function of G_R . The bottom most spectrum is measured from a single phase 1 μm thick $\text{In}_{0.65}\text{Ga}_{0.35}\text{N}$ grown with $G_R = 1.8$ $\mu\text{m}/\text{h}$.

lets and decomposition of InN phase caused by phase separated InGaN. *In situ* monitoring of the surface can thus carry information of when phase separation occurs. The maximum thickness, t_{\max} , of $\text{In}_{0.65}\text{Ga}_{0.35}\text{N}$ alloy that can be grown without phase separation were found to be strongly correlated with G_R . Figure 4(b) shows the variation in t_{\max} with G_R . Maximum thickness increases with G_R with a largest value of $\sim 1.1 \mu\text{m}$ for $\text{In}_{0.65}\text{Ga}_{0.35}\text{N}$ alloy when $G_R = 1.8 \mu\text{m/h}$. Further increase in G_R did not further increase t_{\max} . We believe that as G_R increases, thermodynamic conditions shifted toward more nonequilibriumlike, which promoted the growth of single phase thick layers.

In summary, we have systematically investigated the effects of growth rate on phase separation and the material quality of In-rich InGaN. We found that increasing the growth rate helps to suppressing phase separation and inhomogeneity, thereby improves both the structural and electrical properties of In-rich InGaN epilayers. This and previous studies^{13,20} indicate that growing InGaN alloys far away from the thermodynamic equilibrium conditions (e.g., with higher growth rate) promotes the growth of single phase and improves the material quality of In-rich InGaN epilayers inside the theoretically predicted miscibility gap region. Furthermore, *in situ* interference pattern monitoring also provides an effective tool for directly examining the evolution of phase separation with layer thickness during growth.

This work is supported by NSF (Grant No. DMR-0906879). Jiang and Lin would like to acknowledge the support of Whitacre Endowed Chairs through the AT&T foundation.

¹J. Wu, W. Walukiewicz, K. M. Yu, J. W. Ager III, E. E. Haller, H. Lu, and W. J. Schaff, *Appl. Phys. Lett.* **80**, 4741 (2002).

²J. Wu, W. Walukiewicz, K. M. Yu, J. W. Ager III, E. E. Haller, H. Lu, W. J. Schaff, Y. Saito, and Y. Nanishi, *Appl. Phys. Lett.* **80**, 3967 (2002).

³V. Y. Davydov, A. A. Klochikhin, R. P. Seisyan, and V. V. Emtsev, *Phys. Status Solidi B* **229**, r1 (2002).

⁴O. Jani, I. Ferguson, C. Honsberg, and S. Kurtz, *Appl. Phys. Lett.* **91**, 132117 (2007).

⁵J. Wu, W. Walukiewicz, K. M. Yu, W. Shan, J. W. Ager, E. E. Haller, H. Lu, W. J. Schaff, W. K. Metzger, and S. Kurtz, *J. Appl. Phys.* **94**, 6477 (2003).

⁶R. Dahal, B. Pantha, J. Li, J. Y. Lin, and H. X. Jiang, *Appl. Phys. Lett.* **94**, 063505 (2009).

⁷Y. Nanishi, Y. Satio, and T. Yamaguchi, *Jpn. J. Appl. Phys., Part 1* **42**, 2549 (2003).

⁸C. J. Neufeld, N. G. Toledo, S. C. Cruz, M. Iza, S. P. DenBaars, and U. K. Mishra, *Appl. Phys. Lett.* **93**, 143502 (2008).

⁹B. N. Pantha, R. Dahal, J. Li, J. Y. Lin, H. X. Jiang, and G. Pomrenke, *Appl. Phys. Lett.* **92**, 042112 (2008).

¹⁰K. Aryal, B. N. Pantha, J. Li, J. Y. Lin, and H. X. Jiang, *Appl. Phys. Lett.* **96**, 052110 (2010).

¹¹J. Li, J. Y. Lin, and H. X. Jiang, *Appl. Phys. Lett.* **93**, 162107 (2008).

¹²H. Tong, H. Zhao, V. A. Handara, J. A. Herbsommer, and N. Tansu, *Proc. SPIE* **7211**, 721103 (2009).

¹³B. N. Pantha, J. Li, J. Y. Lin, and H. X. Jiang, *Appl. Phys. Lett.* **93**, 182107 (2008).

¹⁴E. Iliopoulos, A. Georgakilas, E. Dimakis, A. Adikimenakis, K. Tsagaraki, M. Androulidaki, and N. T. Pelekanos, *Phys. Status Solidi A* **203**, 102 (2006).

¹⁵M. Moret, S. Ruffenach, O. Briot, and B. Gil, *Eur. Phys. J.: Appl. Phys.* **45**, 20305 (2009).

¹⁶H. Komaki, R. Katayamac, K. Onabec, M. Ozekib, and T. Ikarib, *J. Cryst. Growth* **305**, 12 (2007).

¹⁷H. J. Kim, Y. Shin, S. Y. Kwon, H. J. Kim, S. Choi, S. Hong, C. S. Kim, J. W. Yoon, H. Cheong, and E. Yoon, *J. Cryst. Growth* **310**, 3004 (2008).

¹⁸S. Nakamura and G. Fasol, *The Blue Laser Diode* (Springer, Berlin, 1997), pp. 201–260.

¹⁹I. Ho and G. B. Stringfellow, *Appl. Phys. Lett.* **69**, 2701 (1996).

²⁰R. Singh, D. Doppalapudi, T. D. Moustakas, and L. T. Romano, *Appl. Phys. Lett.* **70**, 1089 (1997).

²¹C. G. Van de Walle and D. Segev, *J. Appl. Phys.* **101**, 081704 (2007).

²²P. D. C. King, T. D. Veal, C. F. McConville, F. Fuchs, J. Furthmüller, F. Bechstedt, P. Schley, R. Goldhahn, J. Schörmann, D. J. As, K. Lischka, D. Muto, H. Naoi, Y. Nanishi, H. Lu, and W. J. Schaff, *Appl. Phys. Lett.* **91**, 092101 (2007).